



# SEM Analyses of Fossilized Chondrocytes in the Extinct Birds *Yanornis* and *Confuciusornis*: Insights on Taphonomy and Modes of Preservation in the Jehol Biota

Alida M. Bailleul<sup>1,2\*</sup> and Zhonghe Zhou<sup>1,2</sup>

<sup>1</sup>Key Laboratory of Vertebrate Evolution and Human Origins, Institute of Vertebrate Paleontology and Paleoanthropology, Beijing, China, <sup>2</sup>CAS Center for Excellence in Life and Paleoenvironment, Beijing, China

## OPEN ACCESS

### Edited by:

Jasmina Wiemann,  
Yale University, United States

### Reviewed by:

Dawid Michał Surmik,  
University of Silesia, Poland  
Ryan T Tucker,  
Stellenbosch University, South Africa

### \*Correspondence:

Alida M. Bailleul  
alida.bailleul@ivpp.ac.cn

### Specialty section:

This article was submitted to  
Paleontology,  
a section of the journal  
Frontiers in Earth Science

**Received:** 01 June 2021

**Accepted:** 30 July 2021

**Published:** 12 August 2021

### Citation:

Bailleul AM and Zhou Z (2021) SEM Analyses of Fossilized Chondrocytes in the Extinct Birds *Yanornis* and *Confuciusornis*: Insights on Taphonomy and Modes of Preservation in the Jehol Biota. *Front. Earth Sci.* 9:718588. doi: 10.3389/feart.2021.718588

Calcified cartilage is a vertebrate tissue that has unique characteristics, such as a high percentage of calcification, avascularity and cells with apparently delayed autolytic processes after death. All of these factors suggest that fossilized cartilage may be favorable to exceptional cellular preservation, but little is known about chondrocyte fossilization overall in vertebrate paleontology. To further understand the spectrum of cellular preservation in this tissue, we analyze the morphology and the chemistry of some intralacunar content seen in previously published avian cartilage from the Early Cretaceous Jehol biota (in *Yanornis* and *Confuciusornis*). For this, we combine standard paleohistology with Scanning Electron Microscopy (SEM) and Energy Dispersive Spectroscopy (EDS). To better identify some fossilized structures, we compare them with experimentally decayed and biofilm-invaded avian cartilage. Histological images of the cartilage of *Yanornis* show structures that resemble cell nuclei within chondrocyte lacunae. An SEM analysis on this cartilage shows that some lacunae are filled with a type of *in vivo* mineralization (similar to micropetrotic lacunae) and others are filled with small and spherical silicified cells surrounded by an amorphous carbonaceous material. These silicified cells apparently underwent postmortem cell shrinkage and do not constitute cell nuclei. *Confuciusornis* shows filamentous, non-spherical cells that are mostly made of silicon and carbon. This cell morphology does not resemble that of typical healthy chondrocytes, but based on comparison with decaying, biofilm-infiltrated chondrocyte lacunae from extant material, the most plausible conclusion is that the cells of *Confuciusornis* were partially autolyzed prior to their mineralization. In *Yanornis* and *Confuciusornis* respectively, silicification and alumino-silicification were responsible for chondrocyte preservation; while alumino-silicification and ironization occurred in their soft tissues. This shows that alumino-silicification is quite a common mechanism of cellular and soft-tissue preservation in the Jehol biota. Moreover, the two different chondrocyte morphologies (spherical and filamentous) apparently reflect two taphonomical histories, including different timings of postmortem permineralization (one rapid and one much more delayed). This type of analysis paired with more actuataphonomy experiments will be needed in the future to

better understand the preservation potential of chondrocytes and other cell types in the fossil record.

**Keywords:** chondrocytes, cartilage, fossil birds, *Confuciusornis*, *Yanornis*, alumino-silicification, SEM, EDS

## INTRODUCTION

Calcified cartilage, like bone, is a skeletal tissue that can easily fossilize due to its mineralized extracellular matrix (ECM). In fact, the percentage of mineralization is higher in the former than in the latter (e.g., Goret-Nicaise and Dhem, 1985; Jing et al., 2017). However, with the exception of chondrichthyans, cartilage (calcified or uncalcified) is not an abundant tissue in the body of adult vertebrates and is mostly found in embryos. In adults, cartilage is only found as small layers covering bones within joints (e.g., at synovial joints of limb bones, basicranial synchondroses, or joints of the vertebral column) or within some cartilaginous elements that never ossify through ontogeny (e.g., nasal conchae, trachea, larynx), although this can be quite variable across phylogeny. The small amount of cartilage found in the adult vertebrate body when compared to bone is most likely why only few studies in vertebrate paleontology have focused on cartilage so far. Cartilage has been mostly studied in embryonic and juvenile fossil vertebrates. For example, it has helped shed light on interesting aspects of dinosaurian paleobiology, such as the altriciality of *Maiasaura* nestlings, archosaur embryonic growth strategies, or on cranial joint structure and function in nestling dinosaurs (e.g., Horner and Weishampel, 1988; Horner et al., 2001; Bailleul et al., 2012).

In Molecular paleontology, cartilage has also been largely overlooked and only a few studies exist (e.g., Barreto et al., 1993; Jiang et al., 2017). However, a recent study on the cartilage of nestling hadrosaurs (*Hypacrosaurus*) from Montana reported an exquisite histological preservation with cells showing nuclear content such as chromatin threads and circular nuclei (Bailleul et al., 2020a). Due to its mineral:organic ratio, its avascularity and its low levels of oxygen, it was hypothesized that calcified cartilage is a vertebrate tissue that has a great preservation potential for both cells (i.e., for their overall morphological preservation, including that of organelles like nuclei) and for biomolecules (Bailleul et al., 2020a). Additionally, based on published forensics studies on mammalian cartilage, it was hypothesized that chondrocytes can easily be fossilized because their autolysis is apparently naturally delayed after death (Bailleul, 2021). Chondrocytes do not receive nutrition via blood vessels, they are anaerobic and instead receive nutrients via diffusion through the ECM, which makes them resistant to anoxia and acidosis (Rogers et al., 2011; Paulis et al., 2016). A great deal of understanding of this tissue comes from studies on human cadavers and on experimental studies on other mammalian taphonomic models. For example, it was noted that chondrocytes can be viable at ambient temperatures for at least 2 weeks postmortem in cadavers (Lasczkowski et al., 2002) and it has been proposed that chondrocyte viability has the potential to be

used to assess the postmortem interval of human corpses (i.e., the length of time between death and corpse discovery or autopsy performance; e.g., Alibegović, 2014; Bolton, 2015).

All of these data suggest that additional fossil cartilage material should be analyzed to further understand the potential and full spectrum of cellular preservation in this tissue in fossil material. Here, we further investigate cellular preservation (i.e., the morphology of preserved cells and their chemistry) in the calcified cartilage of two fossil birds from the Early Cretaceous Jehol biota of Northeast China. We reanalyze fossilized calcified cartilage that was previously reported on the dentary of *Yanornis* (Bailleul et al., 2019) (Figures 1, 2) and on the furcula of *Confuciusornis* (Wu et al., 2021) (Figures 3, 4). The ground-sections and the content inside the chondrocyte lacunae (i.e., called here intralacunar content) are reanalyzed at higher resolution using scanning electron microscopy (SEM) and Energy Dispersive Spectroscopy (EDS). We also analyze preserved soft tissues in the samples (and compare their chemistry to that of the cells) to better understand the overall taphonomy of the specimens.

## MATERIALS AND METHODS

### Specimens and Gross Morphological Features

We used one specimen of *Yanornis martini* (IVPP V13358) originally described in Zheng et al. 2014 and one specimen of *Confuciusornis* indet. (IVPP V11521) (originally described as *Confuciusornis dui* by Hou et al., 1999). The specimen of *Yanornis* is complete, fully articulated, and well-preserved at the morphological level as it shows evidence of soft tissue remnants like feathers, skin and intestinal content (Zheng et al., 2014). On the other hand, the *Confuciusornis* specimen is incomplete, disarticulated and does not show any evidence of soft-tissue preservation at the morphological level (Hou et al., 1999). We also show one image of calcified cartilage from an extant galliform that was collected as a dry carcass in the field in China (Figure 2C). This specimen was demineralized, processed into paraffin sections and stained with Hematoxylin and Eosin (H&E, see below).

### Paraffin Processing, Embedding and Sectioning of the Extant Galliform

A piece of skull base cartilage attached to subchondral bone was extracted from an extant galliform using a dremel equipped with a rotating blade. The fragment was then fixed in 10% Neutral Buffered Formalin (NBF) for 48 h, then demineralized in a solution of HCl and formic acid (JYBL-II, Cat DD0017,

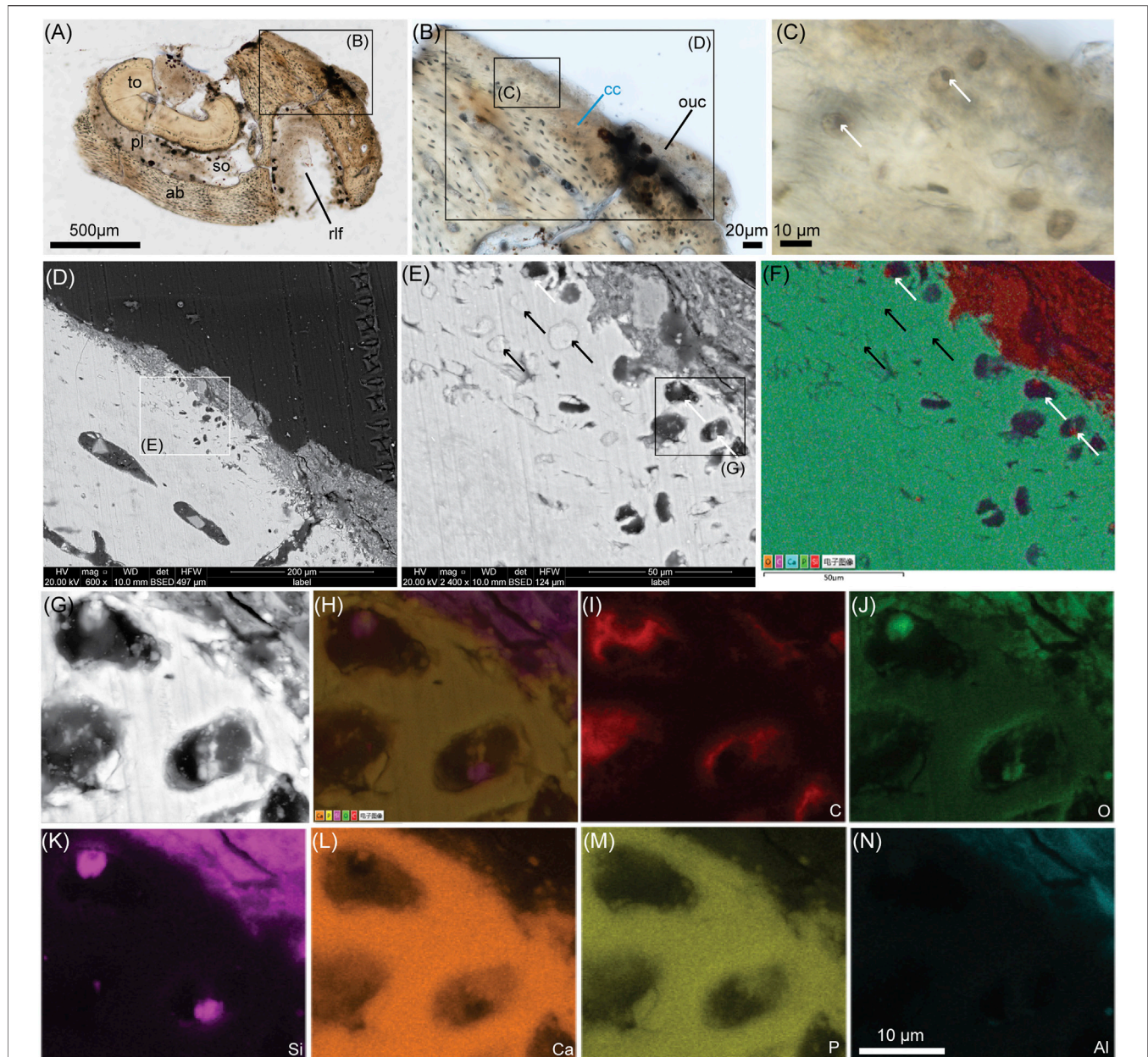


**FIGURE 1** | Ground-section with SEM and EDS analyses of the cartilage on the dentary of *Yanornis* (IVPP V13358). **(A)** Whole-view of a ground section through the rostral-most portion of the dentary of *Yanornis* through the tooth (to) socket (so) and the rostralateral foramina (rif). **(B)** Close-up on symphyseal calcified cartilage (cc) and originally unmineralized cartilage (ouc). **(C)** Close-up on some cc showing round chondrocyte lacunae filled with smaller, dark, spherical material (white arrows) which resemble cell nuclei. **(D)** SEM image of the large rectangle in **(B)**. **(E)** Close-up on the cc from the white square in **(D)**. Some lacunae are filled with white material of the same contrast as the ECM (black arrows) and others are dark and filled with much smaller circular material (white arrows), which are the black spheres seen in **(C)**. **(F)** EDS mapping of the five main chemical elements present in **(E)**. **(G)** Close-up image of some chondrocyte lacunae seen in **(E)**. **(H)** EDS mapping of the five main elements seen in **(G)**. **(I)–(N)** are EDS mapping of the individual elements carbon (C), oxygen (O), silicon (Si), calcium (Ca), phosphorous (P) and aluminum (Al). Additional abbreviations: ab, alveolar bone; cc, calcified cartilage; pl, periodontal ligament. The scale bar is the same from **(G)** through **(N)**.

Leagene) for ~48 h. After demineralization, the extant avian cartilage was subjected to routine dehydration via sequential incubations in 70, 80, 90, 95, and 100% EtOH for ~1 h each. The tissue block was placed in two additional 100% EtOH for 1 h each to ensure complete dehydration, followed by three 30 min

incubations in xylene. Tissues were infiltrated with melted paraffin wax for 30 min each and embedded manually (Paraplast Plus EMS Cat#19216). Blocks were cooled down in an icy water bath and cut on a microtome (Leica Biosystems RM2265), placed in a warm water bath at 44°C with section

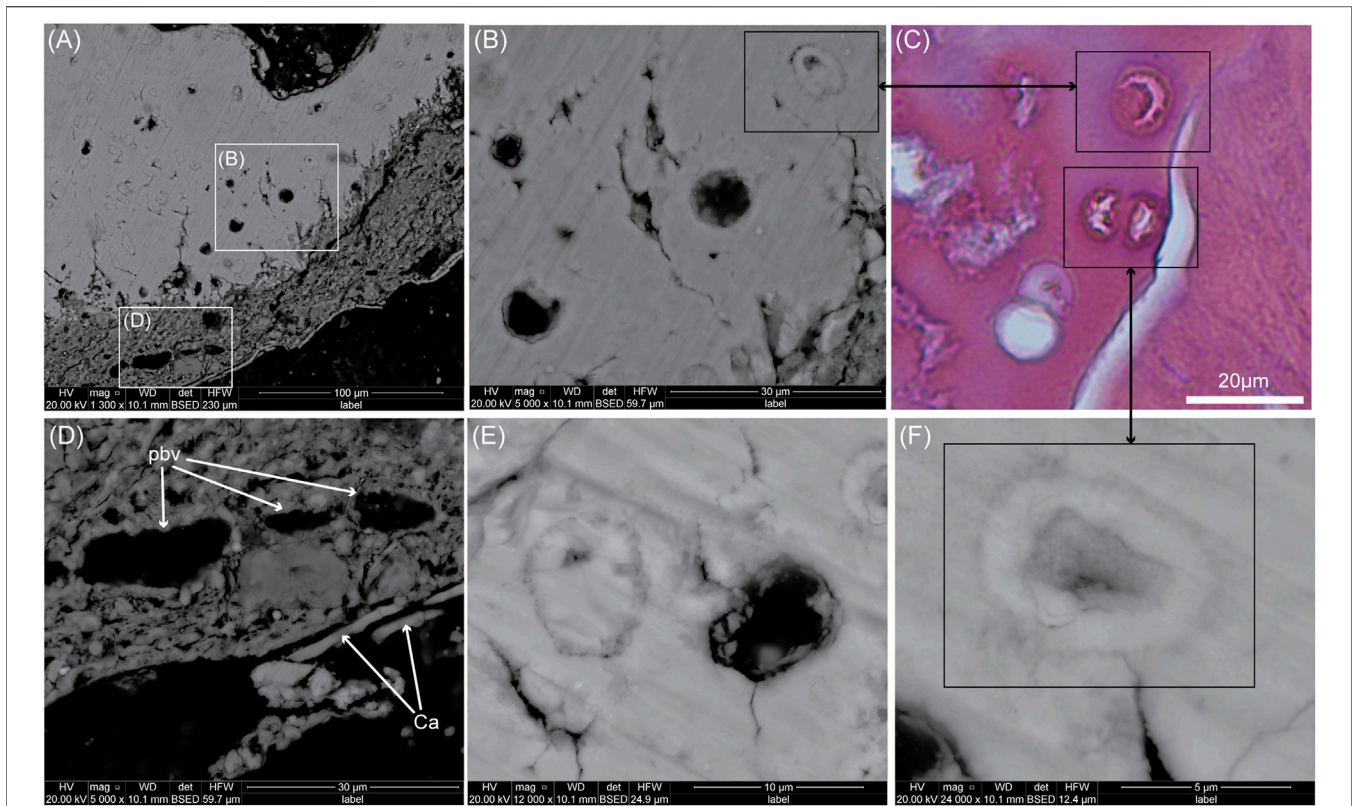


**FIGURE 2** | SEM images of another ground-section of *Yanornis* (IVPP V13358). **(A)** SEM image on the calcified cartilage (upper part) and originally unmineralized cartilage (ouc, lower part). **(B)** Close-up on some chondrocyte lacunae. **(C)** Comparison with a paraffin section of extant galliform calcified cartilage stained with H&E. Some lacunae are being filled in with mineralized material (potentially similar to micropetrotic lacunae seen in mammal bone). They show similar morphologies as those of *Yanornis* (i.e., with a moon-shaped center, or polygonal center). **(D)** Close-up SEM image on the ouc. These tubular structures are potential blood vessels (pbv), meaning the soft tissues originally identified as ouc most likely also contains vascularized collagenous tissues. It is covered by a thin layer of calcium (Ca). **(E)** High-magnification SEM image on two types of chondrocyte lacunae in *Yanornis*. **(F)** High magnification on a micropetrotic chondrocyte lacuna apparently being filled in by calcified matrix perhaps triggered by chondrocyte death and the loss of mineralization inhibitors.

adhesive (Tissue-Grip, StatLab), mounted on charged slides (Superfrost Plus, Fisher Scientific), then dried for a few days at room temperature. Paraffin sections were then deparaffinized with xylene (5 min x 2), rehydrated through a graded EtOH series and stained with H&E (see **Supplementary Data S1.1** for the full staining protocol).

### Paleohistological Ground-Sections

The cartilage on the dentary of *Yanornis* and the furcula of *Confuciusornis* were previously described using ground-sections (see Bailleul et al., 2019 and Wu et al., 2021 for the full protocol for ground-sections). Here, these ground-sections are reanalyzed and photographed under transmitted and/or polarized light using a Nikon eclipse LV100NPOL equipped with a DS-Fi3 camera and the software NIS-Element v4.60. We show two serial ground-sections of *Yanornis* (**Figures 1, 2**) and two in *Confuciusornis* (**Figures 3, 4**).

### SEM-EDS

The ground-sections were also observed using the SEM at the Chinese Academy of Geological Sciences with an FEI Quanta 450

(FEG) at 20 kV. Images are shown in the BSE mode (backscattered electrons). The EDS profiles were measured as maps on the areas that the BSE images captured.

### Actuotaphonomy: Methods for the Observation of the Biofilm Within Decaying Avian Cartilage Under the SEM

This actuotaphonomy experiment and the biofilm were briefly mentioned in a previous study (Bailleul and Li, 2021) but was not fully described. The biofilm was observed in paraffin sections stained with the Gram stain (Microorganism kit Abcam ab245886, which reveals bacteria) (see the **Figures 3A,B** in Bailleul and Li, 2021). In this experiment, the right tibiotarsus of a frozen chicken (a gravid hen) was dissected and left in tapwater for 2 weeks at ambient (summer) temperatures in a Tupperware in oxic conditions near a sunny window in Beijing. After 2 weeks, the decaying and contaminated tibiotarsus was taken out of the water. A piece of cartilage at the proximal surface of the tibiotarsus was dissected and put in NBF for 48 h. It was then demineralized in a solution of HCl and formic acid (JYBL-II,

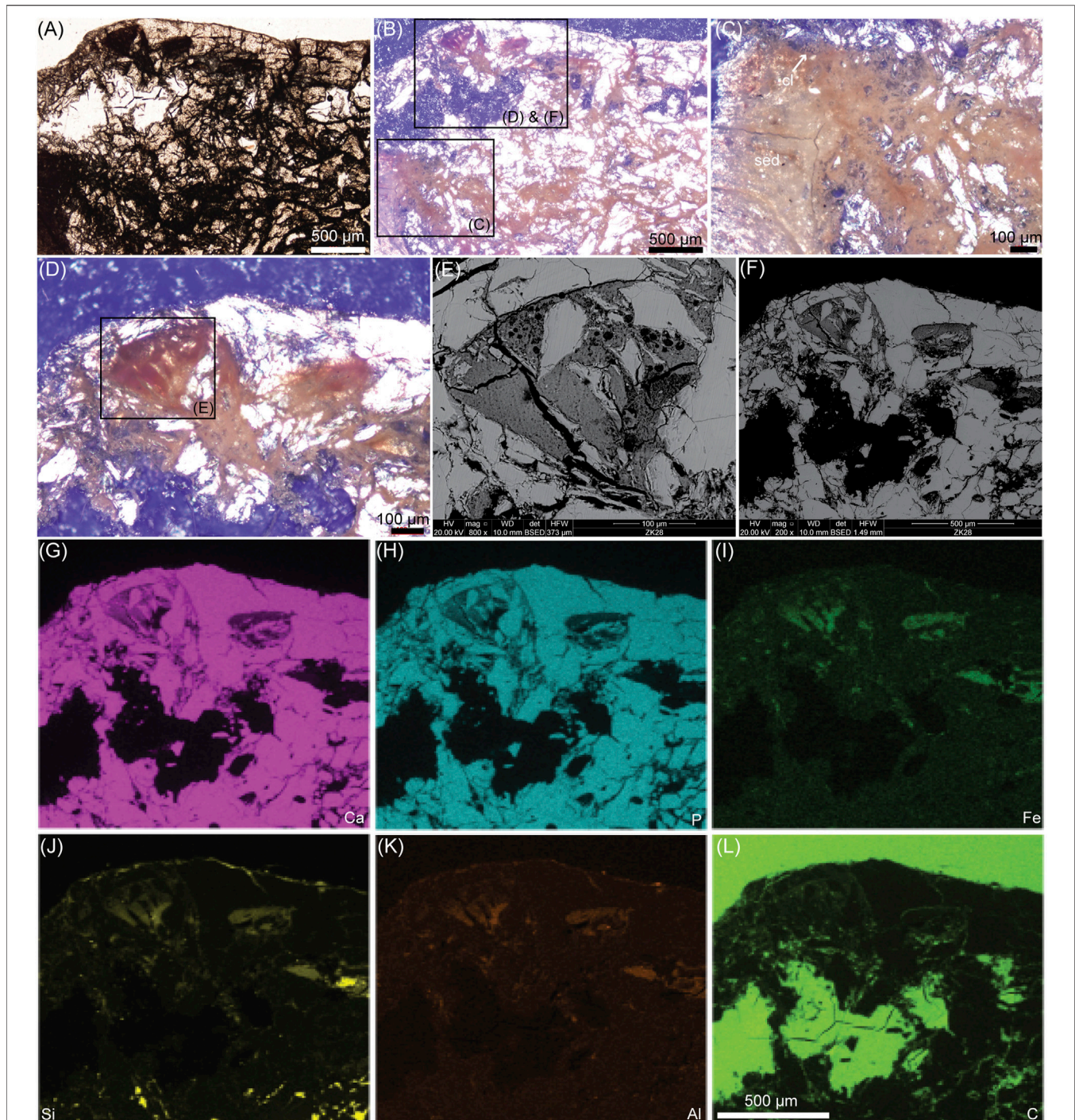


**FIGURE 3** | Ground-section with SEM and EDS analyses of the left epicleideal process of the furcula of *Confuciusornis* (IVPP V11521). **(A)** Photograph of a ground-section under transmitted light. **(B)** Same photograph taken under the polarized light. The entire element is filled with an orangey-brown filamentous network. **(C)** Close-up on that filamentous network, showing the chondrocyte lacunae (cl) are also filled with material of the same color. **(D)** Another close-up showing the filamentous network that is continuous with a darker reddish material inside a vascular space. **(E)** SEM image of tissues seen in a vascular space with no clearly recognizable structure. **(F)** SEM image of **(D)**. **(G)–(L)** are EDS mapping of the individual elements calcium (Ca), phosphorous (P), iron (Fe), silicon (Si), aluminum (Al) and carbon (C). The scale bar is the same from **(G)** through **(L)**. Additional abbreviation: sed, sediment.

Cat DD0017, Leagene) for ~48 h. The fragment was then processed into paraffin slides with the same protocol as the one described above. Some slides were deparaffinized and left

to dry without a coverslip. These deparaffinized sections were sprayed with gold, then observed and photographed rapidly under the SEM. These SEM images were made to observe the

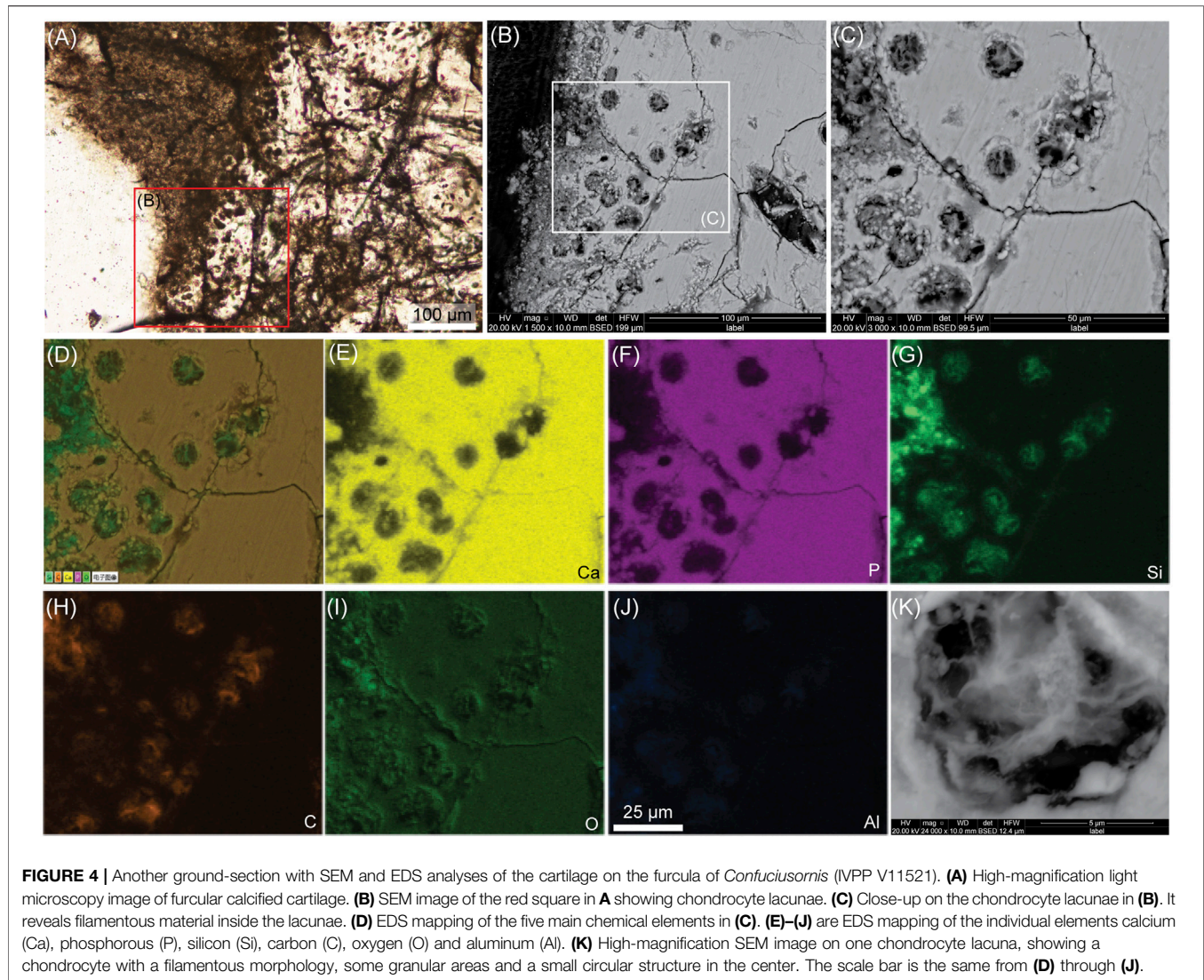


**FIGURE 4 |** Another ground-section with SEM and EDS analyses of the cartilage on the furcula of *Confuciusornis* (IVPP V11521). **(A)** High-magnification light microscopy image of furcular calcified cartilage. **(B)** SEM image of the red square in **A** showing chondrocyte lacunae. **(C)** Close-up on the chondrocyte lacunae in **(B)**. It reveals filamentous material inside the lacunae. **(D)** EDS mapping of the five main chemical elements in **(C)**. **(E)–(J)** are EDS mapping of the individual elements calcium (Ca), phosphorous (P), silicon (Si), carbon (C), oxygen (O) and aluminum (Al). **(K)** High-magnification SEM image on one chondrocyte lacuna, showing a chondrocyte with a filamentous morphology, some granular areas and a small circular structure in the center. The scale bar is the same from **(D)** through **(J)**.

cells and the biofilm invading the decaying cartilage at high resolution (**Figure 5**).

## RESULTS

### ***Yanornis* (IVPP V13358): Calcified Cartilage, Intralacunar Content and Soft Tissues** Previous Histological Descriptions

In the ground-sections of a fragment of the right dentary of IVPP V13358 (**Figures 1A–C**), the bone and the calcified cartilage were well-preserved at the histological level (Bailleul et al., 2019). Both stellate osteocyte lacunae and round chondrocyte lacunae were clearly visible (see the **Figure 3G** in Bailleul et al., 2019). Some chondrocyte lacunae are apparently filled with dark spherical structures (**Figure 1C**, white arrows) and it was hypothesized that they might be remnants of chondrocyte nuclei (Bailleul 2021). The

dentary of IVPP V13358 also preserves soft tissue remnants rich in silicon and aluminum attached to the calcified cartilage and inside the tooth socket (see **Supplementary Figures S6–S7** in Bailleul et al., 2019; also **Figures 1F,K,N** in this study). These soft tissue remnants were respectively hypothesized to be originally unmineralized cartilage ('ouc' in **Figure 1B**) maybe mixed with some collagenous, dense connective tissues of the mandibular symphysis and the originally unmineralized periodontal ligament ('pl' in **Figure 1A**).

### **New SEM and EDS Analyses**

When the calcified cartilage was reanalyzed under the SEM (**Figures 1D,E**), two types of intralacunar content could be seen. The first one shows chondrocyte lacunae filled with a material sharing almost the same appearance as the ECM (black arrows, **Figures 1E,F**). Some of these lacunae are completely filled (**Figure 1E**), others have an outer circular rim with a darker, polygonal center (**Figures 2E,F**) or half-

moon shaped centers (**Figure 2B**). The second type of intralacunar content is characterized by a small white sphere surrounded by a darker and amorphous material (white arrows, **Figures 1E–G**).

EDS mapping on these two types of intralacunar content shows that the lacunae of the first type are filled in with calcium phosphate that has the same chemical composition as the cartilage ECM (**Figure 1F**). The other type of intralacunar content is composed of silicified spherical cores surrounded by a carbonaceous material (**Figures 1F–K**). The soft tissues of *Yanornis* show a composition mostly made of silicon and aluminum (**Figure 1K,N**). Three tubular structures that resemble blood vessels (i.e., most likely venules and not arterioles based on the thickness of the walls) can be seen within the soft tissues attached to the calcified cartilage (**Figure 2D**). Since cartilage is an avascular tissue, these potential blood vessels suggest that this mass of soft tissues does not only contain originally unmineralized cartilage (closest to the calcified cartilage) but also a vascularized, collagenous connective tissue more externally. They are covered by a thin layer mostly made of calcium (**Figure 2D**; **Supplementary Data S1.2**) but to determine exactly what this Ca layer represents is beyond the scope of this paper.

## **Confuciusornis (IVPP V11521): Calcified Cartilage, Intralacunar Content and Soft Tissues**

### **Previous Histological Descriptions**

The histology of the right epicleideal process of the furcula of IVPP V11521 was previously described (Wu et al., 2021). In these sections, the calcified cartilage and bone were not particularly well-preserved and the element showed extensive breakage (and/or compaction of the bony trabeculae on themselves) with a dark color in many places (Wu et al., 2021).

### **Additional Histological Description, SEM and EDS Analyses**

When the element is seen at low magnification with an overexposed polarized light, an orangey-brown network can be seen within all porous spaces and breaks of the furcula (**Figures 3A–D**). This network is continuous with a red-brown material seen in some vascular spaces (**Figure 3D**) and is also found inside the chondrocyte lacunae (**Figure 3C**). The material inside vascular spaces resembles decayed soft tissues (like bone marrow and/or blood breakdown products) under the polarized light (**Figure 3D**), however under the SEM no clearly identifiable tissue or cellular structures can be recognized (**Figure 3E**). The EDS analysis shows that the potential decayed soft tissues and filamentous material are made mostly of iron, silicon, aluminum and some carbon (**Figure 3I–L**).

Under the SEM, high magnification of the chondrocyte lacunae shows that they are filled with a stellate, filamentous material (**Figures 4B,C,K**). Different textures

can be seen within the filamentous material and in one example, one very small circular structure is clear (**Figure 4K**). This stellate morphology is quite different from the round, globular intralacunar content seen in *Yanornis*. EDS shows that the filamentous intralacunar material is mostly made of silicon and carbon, with some aluminum (but no iron) (**Figures 4G,H,J**).

## **DISCUSSION**

### **Identification of the Intralacunar Content in *Yanornis* and *Confuciusornis* *Yanornis* Chondrocytes**

We have described two types of intralacunar content in the calcified cartilage of IVPP V13358 (**Figures 1, 2**). Because the dentary is part of the dermatocranium, this cartilage constitutes secondary cartilage (Bailleul et al., 2019). The two types of intralacunar content could be interpreted as 1) two different types of chondrocytes, or 2) as chondrocytes that underwent two types of postmortem diagenetic alterations. However, based on the EDS mapping (**Figure 1F**) and on comparisons with extant material (**Figure 2C**), we can safely conclude that the intralacunar material made of calcium phosphate does not constitute fossilized chondrocytes but instead a form of *in vivo* intralacunar mineralization. The lacunae of *Yanornis* closely resemble some partially mineralized lacunae observed in the calcified cartilage of extant bird material (in this case, observed in an extant galliform), which shows chondrocyte lacunae in the process of being filled centripetally by ECM (compare **Figure 2F** with **Figure 2C**). One intralacunar filling even shows a moon-shaped center, almost identical to one lacuna seen in *Yanornis* (compare **Figure 2B** with **Figure 2C**). These calcified lacunae are reminiscent of those seen in human bone during micropetrosis, a condition where osteocyte lacunae are mineralized (e.g., Milovanovic et al., 2017). Calcification is initiated by dying osteocytes that release matrix vesicles and apoptotic bodies and concentrate calcified spherites in the lacunae (Milovanovic et al., 2017; Rolvien et al., 2018). In some instances, it is possible that the osteocyte itself mineralizes directly *in situ* with some organelles and potentially nucleic bodies (see Bell et al., 2008, although no mention of the word 'micropetrosis' is made by the authors).

To our knowledge, micropetrotic chondrocyte lacunae have not been reported in any mammalian nor avian material before, but *in vitro* chondrocyte mineralization has been reported in lampreys (Langille and Hall, 1993) and lacunar hypermineralization of intratesseral chondrocytes have been described in extant sharks and rays (Seidel et al., 2016; Seidel et al., 2017). Even though the exact process responsible for chondrocyte lacunae calcification is unknown in extant birds (and therefore also in *Yanornis*), it is possible that, like in human bone, it is the loss of mineralization inhibitors following cell death that induces intralacunar mineralization (Milovanovic et al., 2017; Rolvien et al., 2018). It is quite enigmatic that the

dentary cartilage of *Yanornis* (part of the joint connected with the predeulatory; Bailleul et al., 2019) possesses so many micropetrotic lacunae but investigating this matter is beyond the scope of this paper.

The other type of intralacunar content seen in *Yanornis* shows small silicified spheres within a carbonaceous material. These silicified spheres are numerous and found not just throughout the calcified cartilage matrix but also within the alveolar bone within osteocyte lacunae (see **Supplementary data S1.3**). In this case, the spheres (**Figure 1**) can only represent the actual, original chondrocytes that were permineralized by silicification after the death of IVPP V13358, even though they looked like nuclei in ground-sections based on their size (**Figure 1C**). Like the chondrocytes, the bone cells of this specimen were also silicified (**Supplementary data S1.3**). However, it is unclear what the non-silicified carbonaceous material surrounding the silicified fossil cells represents (**Figure 1I**) and the fact that the cells are much smaller than their lacunae also means cell shrinkage occurred after the death of IVPP V13358. Under normal *in vivo* conditions, healthy cartilage cells fit tightly into their lacunae and the more or less empty lacunar spaces seen in histological sections and SEM preparations of extant cartilage are artefacts associated with fixation and histological processing (e.g., Loqman et al., 2010). Such a processing artefact (cell shrinkage) could not have occurred to these silicified cells. Moreover, tissue and cell distortions mostly occur in demineralized paraffin sections, but not usually in ground-sections.

The cell shrinkage seen in *Yanornis* is therefore difficult to explain. Since IVPP V13358 is complete, articulated and preserves soft tissues at both the morphological and histological level, its burial and permineralization most likely occurred quite rapidly. Moreover, autolytic processes are quite delayed after death in cartilage cells (e.g., Lasczkowski et al., 2002; Rogers et al., 2011; Alibegović, 2014; Bolton 2015; Paulis et al., 2016), therefore it would be expected for the cartilage cells of *Yanornis* to have retained their original size within their lacunae (since it underwent rapid permineralization). To our knowledge, permineralization does not alter cell size nor shape and has not been shown to induce cell shrinkage (e.g., Chen et al., 2009). We can hypothesize that this cell shrinkage may be due to a change in osmolarity (similar to what is seen during dehydration) that occurred prior to silicification, although the clear cause of this change is unknown. Actuataphonomy experiments paired with histological analyses are needed to clarify the cause of postmortem cell size changes. A taphonomy experiment performed on avian cartilage decaying in water showed that the cells that were not attacked by bacteria had no clear size modification after 2 weeks when compared to the cells of the control, fresh tissue (see Bailleul and Li, 2021).

### **Confuciusornis Chondrocytes**

Similarly to the cartilage of *Yanornis*, because the furcula is a membrane bone (originally part of the dermatocranium that got incorporated into the pectoral girdle during evolution; McGonnell, 2001), the furcular cartilage in IVPP V11521 constitutes a secondary cartilage (Wu et al., 2021). One most striking feature in this element is the extensive orangey-brown

network that is seen between bony trabeculae and within chondrocyte lacunae (**Figure 3**). This network apparently constitutes partially decayed soft tissues. It may also be a mix of decayed soft tissues interspersed with a fossilized biofilm. However, under the SEM, the calcified ECM around the chondrocyte lacunae seems intact and no fossilized bacteria can be seen anywhere in the BSE images of this specimen. There is no trace of bacteria penetrating and invading the chondrocyte lacunae. Data from an actuataphonomy experiment on decaying avian cartilage in water for 2 weeks showed the histology of a biofilm invading cartilage (Bailleul and Li, 2021). Here, we show additional images of this biofilm under the SEM (**Figure 5**). It reveals clearly identifiable bacteria that secrete a filamentous sheath of EPS (extracellular polymeric substances) (**Figure 5**). The biofilm is covering a decay-resistant hyaline (uncalcified) cartilage area (**Figure 5A**) and is found within the dissolved matrix of the calcified cartilage (**Figures 5B,C**). Nothing in the SEM images of *Confuciusornis* (**Figures 4B,C**) suggests that it was invaded by a biofilm based on our control extant avian cartilage (**Figure 5**). The only logical explanation is that the intralacunar material represents original chondrocytes, but because they do not resemble healthy chondrocytes, they may have been partially autolyzed prior to permineralization and secondarily obtained this curious filamentous morphology (**Figure 4K**). Additionally, it is also possible that some of the filamentous material may be extracellular coatings that the cells secreted *in vivo*, as is sometimes seen within chondrocyte lacunae in extant cartilage under the SEM (e.g., see **Figure 3D** in Jian et al., 2018; also Clarke, 1974). However, the hypothesis of partially autolyzed cells makes the most sense based on the presence of extensively decayed soft tissues and the clear absence of well-preserved (originally) unmineralized cartilage attached to the calcified cartilage, altogether suggesting that IVPP V11521 underwent extensive decay before or during burial, and that its permineralization was especially delayed.

It is noteworthy that in *Confuciusornis*, the chondrocytes are mostly made of silicon and carbon distributed relatively equally (**Figures 4G,H**); but that in *Yanornis* the carbon was found surrounding the silicified cells (**Figures 1I,K**). These two different patterns are difficult to explain because if the carbonaceous material around the silicified cells in *Yanornis* were fossilized extracellular secretions coating the cells, they should also be silicified. It is possible therefore that the carbonaceous material surrounding the shrunken cells of *Yanornis* are recent contaminants that occurred after ground-sectioning, but this requires further investigation.

### **Silicification, Alumino-Silicification and Diagenetic Precipitation of Iron Oxides in *Yanornis* and *Confuciusornis*: Insights for Cell and Soft-Tissue Preservation in the Jehol Biota**

There are notable differences in the chemistries of the chondrocytes and soft tissues preserved in these two fossils. In *Yanornis*, the chondrocytes were silicified and the soft tissues

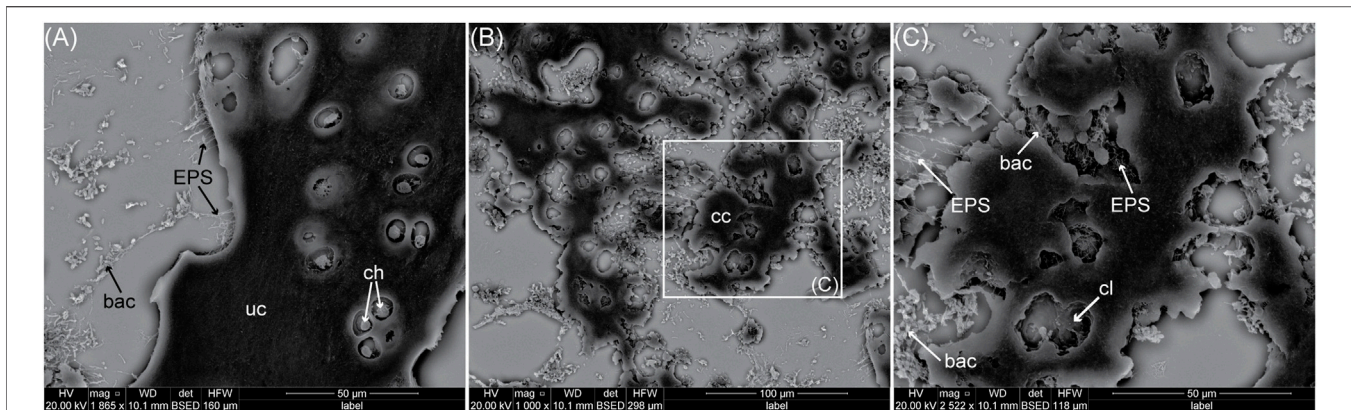


**FIGURE 5** | SEM images (on a gold-sprayed and deparaffinized slide) of a biofilm invasion in decaying avian cartilage in water for 2 weeks. **(A)** Bacterial biofilm on top of uncalcified cartilage (uc). The bacteria (bac) are secreting a sheath of filamentous EPS. The more internal chondrocytes (ch) are intact and not invaded by the biofilm. **(B)** Image in the same sample but within some of the calcified cartilage (cc). The cc has been extensively dissolved. **(C)** Close-up on the dissolved cc showing calcospherites and chondrocyte lacunae (cl) with altered shape. The bacteria and their EPS are infiltrating into the gaps of the dissolved ECM. What caused the dissolution of the calcified ECM is unclear. No clear chondrocyte is visible in these lacunae, meaning they underwent autolysis and/or bacterial attack.

were aluminosilicified (Figure 1). In *Confuciusornis*, chondrocytes were aluminosilicified and the decayed soft-tissues were apparently both aluminosilicified and ironized (most likely by diagenetic precipitation of iron oxides) (Figures 3, 4). This shows that processes of cellular and soft tissue preservation can be different within the same fossil, and demonstrates once again that the chemistry of different fossilized structures that are microns away can be quite different (e.g., see Cadena, 2020).

IVPP V13358 and IVPP V11521 represents additional examples of Jehol fossils where soft-tissues were preserved by aluminosilicification. Tissues forming the remnants of ovarian follicles preserved in the Jehol enantiornithine STM 10–12 (Bailleul et al., 2020b) and the tissues of some Jehol clam shrimp eggs were also aluminosilicified (Pan et al., 2015) showing that aluminosilicification is likely a very common mechanism of soft tissue preservation in the Jehol biota. Unfortunately, little is known about this process of aluminosilicification. It was hypothesized that it is the authigenic precipitation of aluminosilicates from clay minerals that were responsible for the chemistry of the ovarian follicles in enantiornithine STM 10–12 (Bailleul et al., 2020b). In this process, authigenic clays presumably precipitate directly onto tissues (e.g., Gabbott et al., 2001; Martin et al., 2004), but this mechanism seems less plausible for the aluminosilicified chondrocytes of *Confuciusornis* since they are located more internally and protected from sediments within their lacunae. It cannot be ruled out that the chondrocytes were used as a template for clay mineral precipitation, but silicon and aluminum may have also percolated through the fossil in aqueous solutions in a non-crystallized form. Understanding this process of aluminosilicification is beyond the scope of this paper, but the use of methods that can help differentiate amorphous silica from authigenic clay minerals should be encouraged in future taphonomy studies focused on Jehol material.

## SUMMARY AND CONCLUSION

In summary, we have shown that silicification and aluminosilicification are responsible for the preservation of chondrocytes in two avian specimens of the Early Cretaceous Jehol biota. The morphology of the preserved chondrocytes are quite different between *Yanornis* and *Confuciusornis*, which reflects two different taphonomical histories, as well as a process of *in vivo* mineralization (found in *Yanornis* only). In the case of these two fossils, the chondrocytes that retained a round morphology (closer to their *in vivo* shape) are associated with a rapid permineralization after death (in *Yanornis*), whereas the chondrocytes that appear decayed or partially autolyzed are most likely associated with an extensively delayed permineralization (in *Confuciusornis*). Analyzing intralacunar content at high magnification using the SEM helped us differentiate different types of postmortem chondrocyte morphology, processes of cellular preservation and helped us reassess prior hypotheses about the presence of nuclei solely based on ground-sections. The ground-sections of *Yanornis* cartilage in fact do not present chondrocyte nuclei *per se* (as hypothesized in Bailleul, 2021) but instead show shrunken chondrocytes.

In the future, actuataphonomy experiments paired with histology on extant avian material are necessary to 1) further understand processes of postmortem chondrocyte decay (such as cell shrinkage, changes in cell morphology, or the timing of cell autolysis), to 2) clearly differentiate the biotic from the abiotic factors that can affect chondrocyte preservation and 3) to enrich our current understanding of other soft tissues and cell preservation in the fossil record. Viable chondrocytes have the potential to be used to assess the postmortem interval of corpses in forensics (e.g., Alibegović, 2014), and similarly, it is possible that cartilage cell morphology may more or less reflect the postmortem timing of permineralization of a fossil.

## DATA AVAILABILITY STATEMENT

The original contributions presented in the study are included in the article/**Supplementary Material**, further inquiries can be directed to the corresponding author.

## ETHICS STATEMENT

Ethical review and approval was not required for the animal study because we used a cadaveric bird (found already dead by natural causes) and a commercially and legally obtained chicken from a chicken farm.

## AUTHOR CONTRIBUTIONS

AB: designed the study, collected the data, analyzed the data, wrote the paper. ZZ: analyzed the data, contributed to reagents and materials, commented on the paper.

## REFERENCES

- Alibegović, A. (2014). Cartilage: a New Parameter for the Determination of the Postmortem Interval?. *J. Forensic Leg. Med.* 27, 39–45. doi:10.1016/j.jflm.2014.08.005
- Bailleul, A. M. (2021). Fossilized Cell Nuclei Are Not that Rare: Review of the Histological Evidence in the Phanerozoic. *Earth-Science Rev.* 216, 103599. doi:10.1016/j.earscirev.2021.103599
- Bailleul, A. M., Hall, B. K., and Horner, J. R. (2012). First Evidence of Dinosaurian Secondary Cartilage in the Post-Hatching Skull of *Hypacrosaurus Stebingeri* (Dinosauria, Ornithischia). *Plos One* 7 (4), e36112. doi:10.1371/journal.pone.0036112
- Bailleul, A. M., and Li, Z. (2021). DNA Staining in Fossil Cells beyond the Quaternary: Reassessment of the Evidence and Prospects for an Improved Understanding of DNA Preservation in Deep Time. *Earth-Science Rev.* 216, 103600. doi:10.1016/j.earscirev.2021.103600
- Bailleul, A. M., Li, Z., O'Connor, J., and Zhou, Z. (2019). Origin of the Avian Preterminal and Evidence of a Unique Form of Cranial Kinesis in Cretaceous Ornithomorphs. *Proc. Natl. Acad. Sci. USA* 116 (49), 24696–24706. doi:10.1073/pnas.1911820116
- Bailleul, A. M., Zheng, W., Horner, J. R., Hall, B. K., Holliday, C. M., and Schweitzer, M. H. (2020a). Evidence of Proteins, Chromosomes and Chemical Markers of DNA in Exceptionally Preserved dinosaur Cartilage. *Natl. Sci. Rev.* 7 (4), 815–822. doi:10.1093/nsr/nwz206
- Bailleul, A. M., O'Connor, J., Li, Z., Wu, Q., Zhao, T., Monleon, M. A. M., et al. (2020b). Confirmation of Ovarian Follicles in an Enantiornithine (Aves) from the Jehol Biota Using Soft Tissue Analyses. *Commun. Biol.* 3 (1), 1–8. doi:10.1038/s42003-020-01131-9
- Barreto, C., Albrecht, R. M., Bjorling, D. E., Horner, J. R., and Wilsman, N. J. (1993). Evidence of the Growth Plate and the Growth of Long Bones in Juvenile Dinosaurs. *Science* 262 (5142), 2020–2023. doi:10.1126/Science.262.5142.2020
- Bell, L. S., Kayser, M., and Jones, C. (2008). The Mineralized Osteocyte: a Living Fossil. *Am. J. Phys. Anthropol.* 137 (4), 449–456. doi:10.1002/ajpa.20886
- Bolton, S. N. (2015). *Forensic Taphonomy: Investigating the Post Mortem Biochemical Properties of Cartilage and Fungal Succession as Potential Forensic Tools*.
- Cadena, E.-A. (2020). *In Situ SEM/EDS Compositional Characterization of Osteocytes and Blood Vessels in Fossil and Extant Turtles on Untreated Bone Surfaces; Different Preservational Pathways Microns Away*. *PeerJ* 8, e9833. doi:10.7717/peerj.9833

## FUNDING

This work was supported by the National Natural Science Foundation of China (41688103). AMB also thanks CAS-PIFI (Chinese Academy of Sciences-President's International Fellowship Initiative).

## ACKNOWLEDGMENTS

We thank Li Zhiheng for discussions and for collecting the extant galliform and Zhang Shukang for making the ground-sections.

## SUPPLEMENTARY MATERIAL

The Supplementary Material for this article can be found online at: <https://www.frontiersin.org/articles/10.3389/feart.2021.718588/full#supplementary-material>

- Chen, X., Wang, W., Shang, Q., Lou, Y., Liu, X., Cao, C., et al. (2009). Experimental Evidence for Eukaryotic Fossil Preservation: Onion Skin Cells in Silica Solution. *Precambrian Res.* 170 (3–4), 223–230. doi:10.1016/j.precamres.2009.01.006
- Clarke, I. C. (1974). Articular Cartilage: a Review and Scanning Electron Microscope Study. II. The Territorial Fibrillar Architecture. *J. Anat.* 118 (Pt 2), 261–280.
- Gabbott, S. E., Norry, M. J., Aldridge, R. J., and Theron, J. N. (2001). Preservation of Fossils in clay Minerals; a Unique Example from the Upper Ordovician Soom Shale, South Africa. *Proc. Yorkshire Geol. Soc.* 53 (3), 237–244. doi:10.1144/pygs.53.3.237
- Goret-Nicaise, M., and Dhem, A. (1985). Comparison of the Calcium Content of Different Tissues Present in the Human Mandible. *Cells Tissues Organs* 124 (3–4), 167–172. doi:10.1159/000146113
- Horner, J. R., Padian, K., and de Ricqlès, A. (2001). Comparative Osteohistology of Some Embryonic and Perinatal Archosaurs: Developmental and Behavioral Implications for Dinosaurs. *Paleobiology* 27 (1), 39–58. doi:10.1666/0094-8373(2001)027<0039:coosea>2.0.co;2
- Horner, J. R., and Weishampel, D. B. (1988). A Comparative Embryological Study of Two Ornithischian Dinosaurs. *Nature* 332 (6161), 256–257. doi:10.1038/332256a0
- Hou, L., Martin, L. D., Zhou, Z., Feduccia, A., and Zhang, F. (1999). A Diapsid Skull in a New Species of the Primitive Bird *Confuciusornis*. *Nature* 399 (6737), 679–682. doi:10.1038/21411
- Jian, Q.-L., HuangFu, W.-C., Lee, Y.-H., and Liu, I.-H. (2018). Age, but Not Short-Term Intensive Swimming, Affects Chondrocyte Turnover in Zebrafish Vertebral Cartilage. *PeerJ* 6, e5739. doi:10.7717/peerj.5739
- Jiang, B., Zhao, T., Regnault, S., Edwards, N. P., Kohn, S. C., Li, Z., et al. (2017). Cellular Preservation of Musculoskeletal Specializations in the Cretaceous Bird *Confuciusornis*. *Nat. Commun.* 8, 14779. doi:10.1038/ncomms14779
- Jing, Y., Jing, J., Ye, L., Liu, X., Harris, S. E., Hinton, R. J., et al. (2017). Chondrogenesis and Osteogenesis Are One Continuous Developmental and Lineage Defined Biological Process. *Scientific Rep.* 7 (1), 1–10. doi:10.1038/s41598-017-10048-z
- Langille, R. M., and Hall, B. K. (1993). Calcification of Cartilage from the Lamprey *Petromyzon Marinus* (L.) *In Vitro*. *Acta Zoologica* 74 (1), 31–41. doi:10.1111/j.1463-6395.1993.tb01218.x
- Lasczkowski, G. E., Aigner, T., Gamberdinger, U., Weiler, G., and Bratzke, H. (2002). Visualization of Postmortem Chondrocyte Damage by Vital Staining and Confocal Laser Scanning 3D Microscopy. *J. Forensic Sci.* 47 (3), 663–666. doi:10.1520/jfs2000258
- Loqman, M., Bush, P. G., Farquharson, C., and Hall, A. (2010). A Cell Shrinkage Artefact in Growth Plate Chondrocytes with Common Fixative

- Solutions: Importance of Fixative Osmolarity for Maintaining Morphology. *eCM* 19, 214–227. doi:10.22203/ecm.v019a21
- Martin, D., Briggs, D. E. G., and Parkes, R. J. (2004). Experimental Attachment of Sediment Particles to Invertebrate Eggs and the Preservation of Soft-Bodied Fossils. *J. Geol. Soc.* 161 (5), 735–738. doi:10.1144/0016-764903-164
- McGonnell, I. M. (2001). The Evolution of the Pectoral Girdle. *J. Anat.* 199 (1-2), 189–194. doi:10.1046/j.1469-7580.2001.19910189.x
- Milovanovic, P., Zimmermann, E. A., Vom Scheidt, A., Hoffmann, B., Sarau, G., Yorgan, T., et al. (2017). The Formation of Calcified Nanospherites during Micropetrosis Represents a Unique Mineralization Mechanism in Aged Human Bone. *Small* 13 (3), 1602215. doi:10.1002/smll.201602215
- Pan, Y., Wang, Y., Sha, J., and Liao, H. (2015). Exceptional Preservation of Clam Shrimp (Branchiopoda, Eucrustacea) Eggs from the Early Cretaceous Jehol Biota and Implications for Paleoecology and Taphonomy. *J. Paleontol.* 89 (3), 369–376. doi:10.1017/jpa.2015.24
- Paulis, M., Hassan, E., and Abd-Elgaber, N. (2016). Estimation of Postmortem Interval from Cartilage Changes of Rabbit Auricle. *Ain Shams J. Forensic Med. Clin. Toxicol.* 26 (1), 61–69. doi:10.21608/ajfm.2016.18545
- Rogers, C. J., Clark, K., Hodson, B. J., Whitehead, M. P., Sutton, R., and Schmerer, W. M. (2011). Postmortem Degradation of Porcine Articular Cartilage. *J. forensic Leg. Med.* 18 (2), 52–56. doi:10.1016/j.jflm.2010.11.006
- Rolvien, T., Riedel, C., Milovanovic, P., Jeschke, A., Butscheidt, S., Poeschel, K., et al. (2018). “Accelerated Bone Aging in Human Auditory Ossicles Is Accompanied by Excessive Hypermineralization, Osteocyte Death and Micropetrosis,” in *Journal of Bone and Mineral Research* (NJ USA: WILEY 111 RIVER ST, HOBOKEN 07030-5774), S353.
- Seidel, R., Blumer, M., Pechriggl, E.-J., Lyons, K., Hall, B. K., Fratzl, P., et al. (2017). Calcified Cartilage or Bone? Collagens in the Tessellated Endoskeletons of Cartilaginous Fish (Sharks and Rays). *J. Struct. Biol.* 200 (1), 54–71. doi:10.1016/j.jsb.2017.09.005
- Seidel, R., Lyons, K., Blumer, M., Zaslansky, P., Fratzl, P., Weaver, J. C., et al. (2016). Ultrastructural and Developmental Features of the Tessellated Endoskeleton of Elasmobranchs (Sharks and Rays). *J. Anat.* 229 (5), 681–702. doi:10.1111/joa.12508
- Wu, Q., O'Connor, J. K., Li, Z.-H., and Bailleul, A. M. (2021). Cartilage on the Furculae of Living Birds and the Extinct Bird *Confuciusornis*: A Preliminary Analysis and Implications for Flight Style Inferences in Mesozoic Birds. *Vertebrata Palasiatica* 59 (2), 106. doi:10.19615/j.cnki.1000-3118.201222
- Zheng, X., O'Connor, J. K., Huchzermeyer, F., Wang, X., Wang, Y., Zhang, X., et al. (2014). New Specimens of *Yanornis* Indicate a Piscivorous Diet and Modern Alimentary Canal. *PLoS One* 9 (4), e95036. doi:10.1371/journal.pone.0095036

**Conflict of Interest:** The authors declare that the research was conducted in the absence of any commercial or financial relationships that could be construed as a potential conflict of interest.

**Publisher's Note:** All claims expressed in this article are solely those of the authors and do not necessarily represent those of their affiliated organizations, or those of the publisher, the editors and the reviewers. Any product that may be evaluated in this article, or claim that may be made by its manufacturer, is not guaranteed or endorsed by the publisher.

Copyright © 2021 Bailleul and Zhou. This is an open-access article distributed under the terms of the Creative Commons Attribution License (CC BY). The use, distribution or reproduction in other forums is permitted, provided the original author(s) and the copyright owner(s) are credited and that the original publication in this journal is cited, in accordance with accepted academic practice. No use, distribution or reproduction is permitted which does not comply with these terms.